ISSN 1990-7478, Biochemistry (Moscow) Supplement Series A: Membrane and Cell Biology, 2008, Vol. 2, No. 1, pp. 73–81. © Pleiades Publishing, Ltd., 2008.
Original Russian Text © K.V. Shaitan, M.Yu. Antonov, Ye.V. Tourleigh, O.V. Levtsova, K.B. Tereshkina, I.N. Nikolaev, M.P. Kirpichnikov, 2008, published in Biologicheskie Membrany, 2008, Vol. 25, No. 1, pp. 66–75.

Comparative Study of Molecular Dynamics, Diffusion, and Permeability for Ligands in Biomembranes of Different Lipid Composition

K. V. Shaitan[a], M. Yu. Antonov[a, b], Ye. V. Tourleigh[a], O. V. Levtsova[a], K. B. Tereshkina[a], I. N. Nikolaev[b], and M. P. Kirpichnikov[a]

[a] *Lomonosov Moscow State University, Moscow, 119991 Russia*
e-mail: shaitan@moldyn.org, mikhail@moldyn.org, yegor@moldyn.org,
[b] *Ammosov Yakut State University, ul. Belinskogo 58, Yakutsk, 677000 Russia*
e-mail: n_ivan_n@mail.ru

Received August 21, 2007

Abstract—A comparative study of several model lipid bilayers of different composition, which included analysis of kinetic parameters of model lipid bilayers and permeability of bilayer membranes for small molecules, has been carried out. The conformity of results of numeric experiments to experimental data (structure of membrane lipid bilayers, lateral diffusion coefficients, and relative permeability of biomembranes for ligands) is discussed in the framework of a standard molecular dynamics protocol.

DOI: 10.1134/S199074780801011X

Structural and kinetic properties of biological membranes play a crucial role in cell-mediated processes [1]. In this context, simulation of biomembrane structures by the steered molecular dynamics (MD) method presents considerable interest in view of rapid progress in molecular and membrane technologies [2] and unique opportunities for detailing and visualization of molecular processes in complexly built structures on the basis of advanced numeric experiment protocols [3–5]. The latter includes microscopic mass transfer imaging in strongly anisotropic and complexly structured media, diffusion at membrane/water interface, formation and relaxation of non-equilibrium heterophasic systems, etc. [6, 7].

The use of MD simulation in membrane studies [8, 9] is often coupled with considerable difficulties. As molecular models of membrane structures contain no less than 10^4 atoms, calculation of 100-ns trajectories in all-atom force fields is tedious and time-consuming. Moreover, characteristic times of passive ion transport are usually measured on a microsecond scale. Therefore, a search for novel efficient numeric protocols for obtaining explicit information in a reasonably short time is a currently central task. Several approaches to the solution of this problem exist, but a simple two-phase solvation model for fast assessment of miscellaneous effects of hydrophobicity factors on structural interfacial changes in biomolecules [10, 11] seems to be more preferable. However, this approach has one serious disadvantage, viz., it does not take into account the contribution of Coulomb interactions between membrane components and ligands. Coarse-grained simulations of membrane lipid bilayers [12] notably reduce the experimental time, but fail to provide reliable kinetic information even when sophisticated heavy-atom lipid bilayer models are used [13, 14]. Of course, nearly all specific simulated structures can be calibrated in such a way that some calculated parameters are brought in full conformity with experimental data, but versatility of MD protocols and possibility to extend them to other objects leave doubt. At the same time, MD simulation of hydrated lipid bilayers of 1-palmitoyl-2-oleoyl-*sn*-glycero-3-phosphatidylcholine (POPC) culminated in the development of a novel efficient MD protocol. This procedure is based on all-atom Amber 1999 force field [15] and is designed for the study of major structural and kinetic parameters of biomembranes. The main feature of the novel approach is to bring the system to a state characterized by equilibrium distribution of fluctuations of major macroparameters, such as temperature, volume, pressure, etc. [16, 17]; its practical utility consists in broadening the range of objects analyzed by the method in question and bringing experimental values of lateral pressure to conformity with previously obtained data [18].

This study is an overview of structural regularities and dynamic behavior of lipid membranes whose lipid compositions are similar to those of higher organisms in the example of three most common membrane lipids and their bilayers with special reference to permeability of biomembranes for low-molecular endogenous ligands. Physical mechanisms of these processes are still poorly understood despite the large body of evidence on permeability of biomembranes for low-

Table 1. Values of lateral pressure for Systems I–III

System	Mean specific area, Å^2	Lateral pressure, bar
I	78.0 ± 5.5	–242
II	65.4 ± 1.5	–300
III	66.8 ± 3.7	–265

Table 2. Calculated values of specific area, bilayer thickness, and isothermal compression coefficients

System	Mean membrane thickness, Å	χ_T, Pa^{-1}
I	34.33 ± 0.39	1.7×10^{-10}
II	35.54 ± 0.25	1.4×10^{-10}
III	36.06 ± 0.32	2.1×10^{-10}

molecular solutes [19]. In this study, the steered MD (SMD) simulation was used as a method of choice in the analysis of permeabilities of biomembranes for ligands [16, 17, 20, 21]. The procedure consists in applying external force to the ligand and steering the system through a definite evolutional scenario, i.e., monitoring of transmembrane transport even in relatively short trajectories and estimation of parameters which are characteristic for ligand translocation.

EXPERIMENTAL

The following models of bilayer lipid membranes of different lipid composition were used: 1-palmitoyl-2-oleoyl-*sn*-glycero-3-phosphatidylcholine (POPC), 1,2-dipalmitoyl-*sn*-glycero-3-phosphatidylcholine (DPPC) and 1,3-(1-stearoyl-2-palmitoyl-*sn*-glycero-3-phosphatidyl)glycerol (cardiolipin, CL). Their trajectories were calculated using a package of molecular dynamics programs (PUMA software) [22, 23]. Classical equations were solved with the help of Verlet algorithm with the Amber 1999 potential field [15].

The calculations were carried out under periodic boundary conditions for three hydrated lipid bilayers: (i) 8 CL molecules, 16 POPC molecules, and 16 DPPC molecules (System I); (ii) 30 POPC molecules and 30 DPPC molecules (System II) and (iii) 64 POPC molecules (System III). The original structures of the lipid bilayers corresponded to the perpendicular position of the principal axis relative to the plane of the membrane. To achieve this, prior to experiments lipid molecules were turned round the long axis to a random angle. For each lipid molecule, there were 34–43 solvent molecules; in the majority of lipids full hydration is reached only when no less than 27 water molecules per one lipid is used [24]. In the initial configuration, water molecules were separated from extreme atoms by a distance no less than 2.3 Å. The original design of the experimental systems afforded full conformity of their specific areas to calculated values [25–30], e.g., 62–68 Å^2 for POPC, 59–62 Å^2 for DPPC, and 100–120 Å^2 for CL. In bilayers formed from different lipids, specific areas were calculated as mean areas of participating lipids relative to their concentration.

Partial charges and force constants for lipid molecules were calculated as described previously [16]. The negative charge of CL molecules (–2) was compensated by adding Na^+ ions to water. The valence bonds and valence angles in water molecules were not fixed (TIP3P model). The van der Waals interactions were analyzed using a special smoothed (switching) function. The value of the Coulomb potential was multiplied by a special shielding function as described in [16]. The value of the cut-off radius for Coulomb interactions varied from 16 to 20 Å depending on membrane type. The value of the dielectric constant was taken equal to unity; the numerical integration step was 1 fs.

The calculations were performed under periodic boundary conditions at constant temperature and under constant pressure (*NPT* ensemble). Barostating was performed in a Berendsen altitude chamber; the relaxation time (100 ps) was the same in all directions. To ensure conformity of the specific area of the lipid bilayer to experimental values [25–30] and to take into consideration the contribution of surface tension of the lipid bilayer, the lateral components of pressure were taken negative [31]. Constant temperature (300 K) was maintained with the help of a collisional medium (collisional thermostat [23]). Mean collision frequency of virtual particles was 10 ps^{-1}; average particles mass was 1 a.m.u.

RESULTS AND DISCUSSION

In the first series of our experiments, we studied lipid bilayer relaxation (200–500 ps, 500 K) and selected a working part in the MD trajectory no less than 2 ns long.

In studies of dynamics, negative lateral pressure was applied to the test systems in order to maintain mean specific area close to initial level (Table 1).

Figures 1a–1c show probability densities of volume fluctuations of a calculation cell for the systems considered. As can be seen, the probability density of these fluctuations had the shape of a Gaussian distribution. In terms of Einstein thermodynamic fluctuation theory, the probability density of equilibrium fluctuations of volume $p(\Delta V)$ is set by the Gaussian distribution:

$$p(\Delta V) = A_V e^{-\frac{(\Delta V)^2}{2\langle \Delta V^2 \rangle}}.$$

The figures in broken brackets $\langle\ \rangle$ represent the derivation of the mean, A_V is the normalization factor, $\langle \Delta V^2 \rangle = k_b T V \chi_T$ is the dispersion and χ_T is the isothermal compression coefficient for the given system. Hence, the value of $\langle \Delta V^2 \rangle$ was obtained after calculation of χ_T (Table 2). Previous studies showed that χ_T for

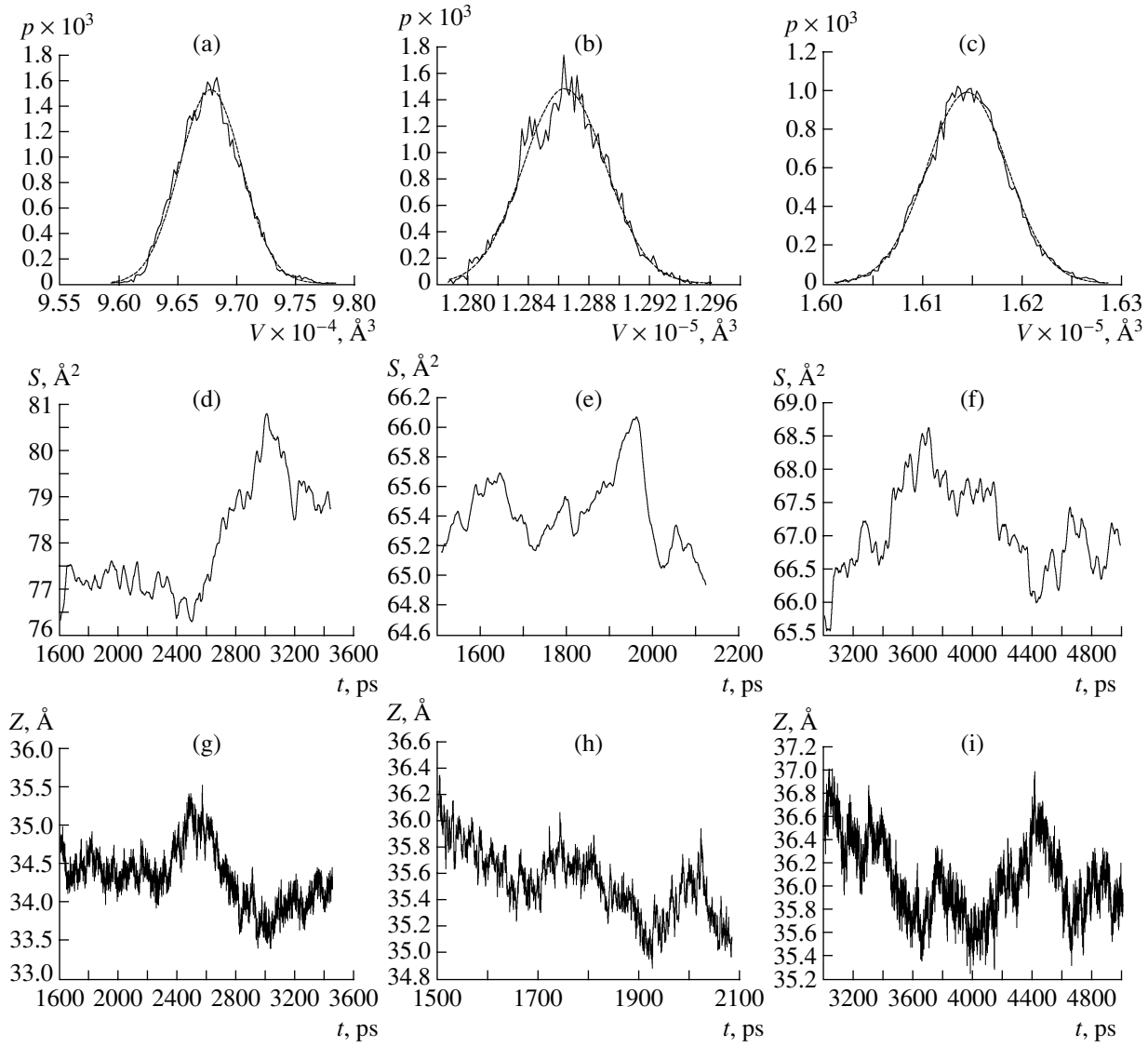

Fig. 1. Parameters of the calculation cell. (a–c) Probability density of calculation cell volume and Gaussian approximation of the experimental curve. (d–f) Specific area fluctuations per lipid molecule. (g–i) Bilayer thickness fluctuations for Systems I–III, respectively.

lipid membranes lies in the range from 1×10^{-10} to 6×10^{-10} Pa^{-1} [32]. The experimental values of χ_T also lie within a reasonable range.

Membrane thickness (Figs. 1g–1i) was defined as a distance between phosphorus atoms in adjacent monolayers. Their mean values are listed in Table 2.

Figure 2 shows the mean-square deviation and linear approximation of displacement of POPC molecules for different experimental systems. The lateral diffusion coefficient of the lipids D_{xy} is defined as a linear approximation coefficient for the dependence:

$$\langle (x(t+\tau) - x(t))^2 + (y(t+\tau) - y(t))^2 \rangle = 4D_{xy}t.$$

Here, the square deviation of the mass center of a lipid in the plane of the lipid bilayer is put in broken brackets. The averaging was performed individually for each lipid type: $0 < t < T - \tau$ ps, $0 < \tau < 300$ ps, where T is the length of the working part of the trajectory.

The calculated values of D_{xy} (Table 3) were close to those for quasi-elastic neutron scattering on DPPC (1×10^{-7} cm^2/s, [33]) and dioleoylphosphatidylcholine (2×10^{-7} cm^2/s, [34]) bilayers. The corresponding values obtained after pulse-modulated NMR of POPC bilayers at 298 and 303 K were 2.0×10^{-7} and 2.5×10^{-7} cm^2/s, respectively [35]. Comparison of results obtained for times lesser than 1 ns to neutron scattering data is more correct, since at higher (1 ns) values of this parameter diffusion induces more profound changes in the membrane structure (10 Å) [36], while diffusion coefficients measured by fluorescent methods are 2–

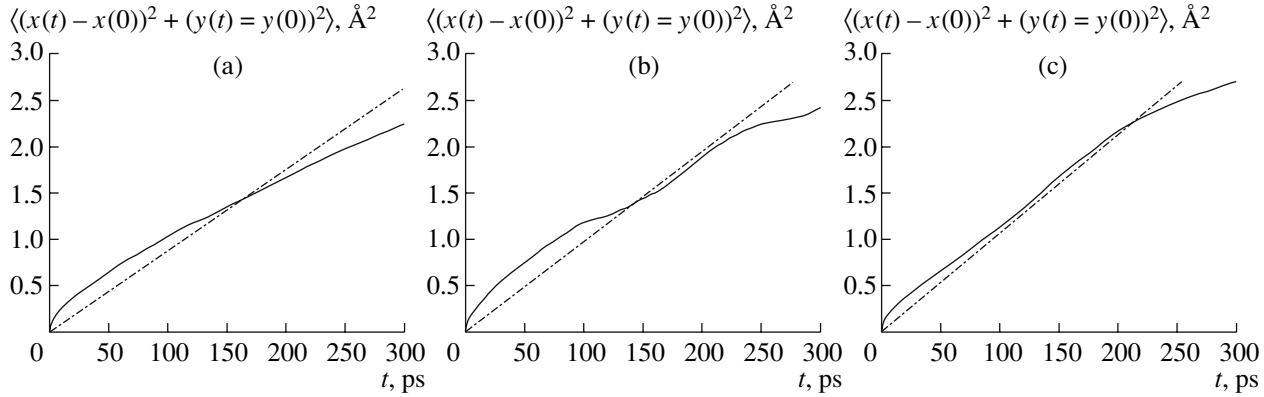

Fig. 2. Mean area of POPC geometric center translocation in the plane of the lipid bilayer and its linear approximation for Systems I (a), II (b) and III (c).

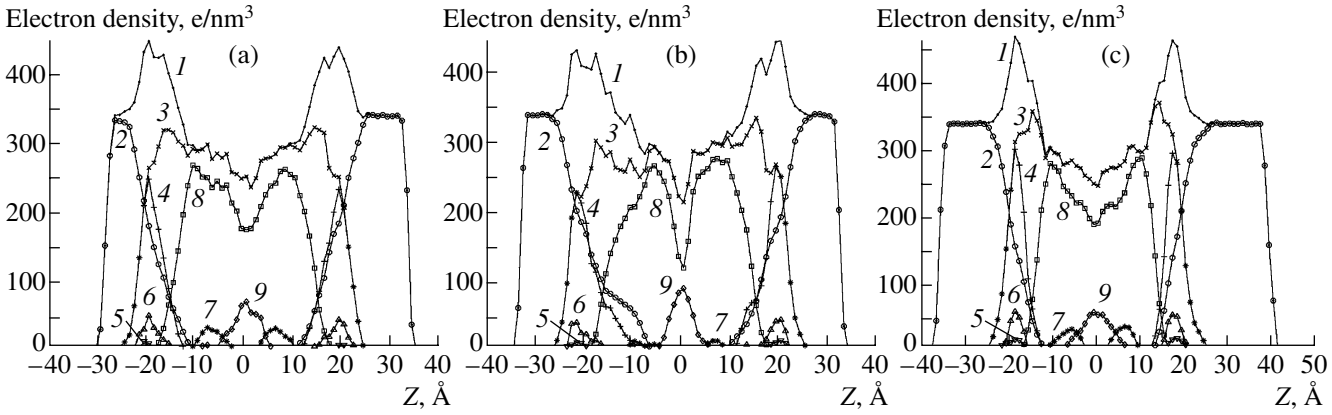

Fig. 3. Distribution of electron density in Systems I (a), II (b) and III (c). Curve *1*, integral system; *2*, water; *3*, lipid; *4*, lipid heads; *5*, nitrogen atoms; *6*, phosphorus atoms; *7*, HC=CH-groups; *8,* CH_2 groups of alkyl chains; *9*, terminal CH_3-group of alkyl chains.

3 times as low [37]. Direct comparison is hardly efficient under these conditions, since lipid translocation can be impeded by the label (e.g., rhodamine).

After introduction of a double *cis*-bond (POPC) or an increase in the molecular size (POPC and CL), the lateral mobility of the lipid bilayer descends, weakly but steadily, in the following order: DPPC ⟶ POPC ⟶ CL. At the same time, low sensitivity of the lateral diffusion coefficient to the structure of the lipid membrane suggests that the mechanism of lateral diffusion is confined to gradual small-scale displacement of individual components of the lipid membrane and does not involve the whole lipid molecule.

Table 3. Calculated values of lateral diffusion coefficients

System	Lipid	D_{xy}, cm^2/s	Experimental value, cm^2/s
I	POPC	$(2.2 \pm 0.3) \times 10^{-7}$	–
I	DPPC	$(2.2 \pm 0.5) \times 10^{-7}$	–
I	CL	$(2.0 \pm 0.3) \times 10^{-7}$	–
II	POPC	$(2.4 \pm 0.6) \times 10^{-7}$	–
II	DPPC	$(2.6 \pm 0.7) \times 10^{-7}$	1×10^{-7}* [33]
III	POPC	$(2.6 \pm 0.5) \times 10^{-7}$	$(2.0–2.5) \times 10^{-7}$ [35]

* For monolipid bilayers.

Matching of other critical parameters of model lipid bilayers also takes place. This concerns, in particular, distribution of averaged electron and atomic group densities along the normal to the membrane. Similar dependences were established for, e.g., DPPC [38], dioleoylphosphatidylcholine [39] and POPC [28]. The distribution of electron density in membranes of different lipid composition is shown in Fig. 3.

In another series of our experiments, we investigated radial atomic distribution $g(r)$ in the plane of the lipid membrane. The function $g(r)$ determines the probability of localization of a certain group of atoms at a definite distance from other atoms projected onto the plane of the membrane. The number of atoms dN in the circular layer with the square dS and thickness dr, which is separated by a distance r from the central atom

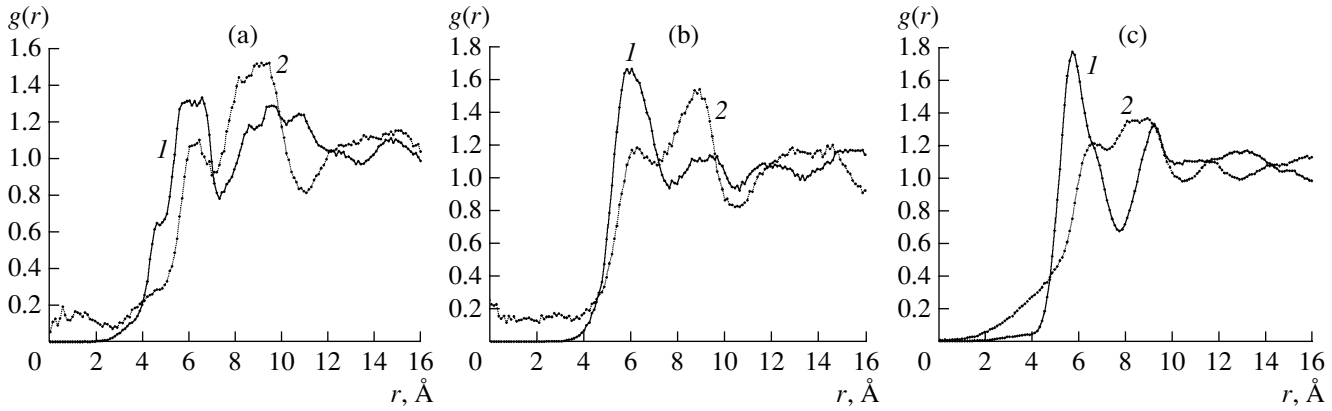

Fig. 4. Radial distribution functions of nitrogen and phosphorus atoms in the plane of the membrane for Systems I (a), II (b) and III (c); *1*, P–P; *2*, N–N.

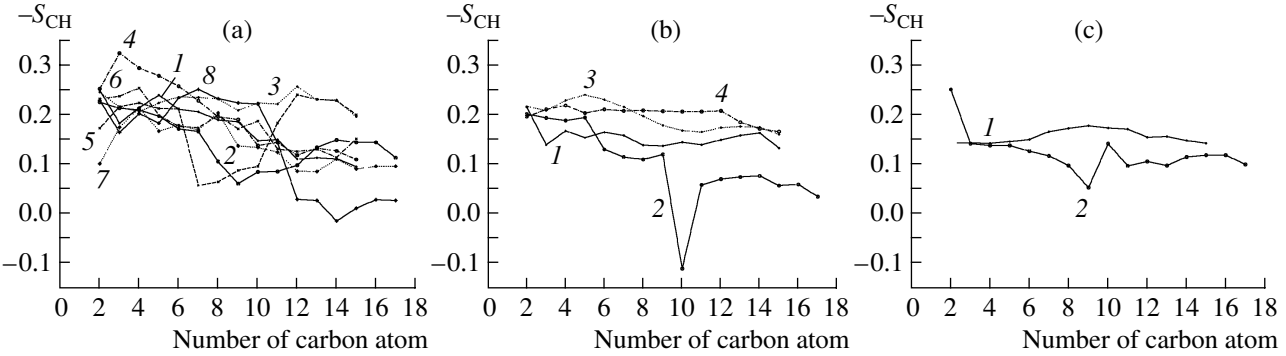

Fig. 5. Profiles of order parameters for C–H-bonds in the alkyl chains of Systems I (a), II (b), and III (c). *1*, Palmitoyl chains of POPC; *2*, oleoyl chains of POPC; *3* and *4*, palmitoyl chains of DPPC; *5* and *6*, palmitoyl chains of CL; *7* and *8*, stearoyl chains of CL.

(where N is the total number of atoms of the given type), is correlated with $g(r)$ as:

$$dN = Ng(r)\frac{dS}{S} = \frac{N}{S}g(r)2\pi r dr.$$

The radial distribution of phosphorus and nitrogen atoms in the plane of the membrane is shown in Fig. 4; the averaging was performed for the both lipid layers. The radial distribution patterns of nitrogen atoms testify to close-spaced localization of nitrogen atoms around the lipid heads of the membrane lipid bilayer, especially if such membranes contain different types of lipids. The thickness of the hydrophilic lipid bilayer is such that weakly charged, mutually repulsive nitrogen atoms are localized at different depths in the membrane lipid bilayer. Actually, heavily charged phosphorus atoms cannot be separated from one another by such a short distance. The magnitude of the first maximum diminishes with the increase in the number of bilayer lipid types as a result of which the orderliness of the lipid bilayer is impaired even if the distance between the atoms is small. In our study, the shapes of the experimental curves testify to the lack of long-range packing of membrane lipid heads (Fig. 4).

The values of the order parameter S_{CH} (Fig. 5), which can be established by NMR spectroscopy of deuterated lipids, were calculated from MD data. Averaged values of this parameter can also be calculated from IR spectroscopic data [6]. The order parameter for the C–H bonds in the alkyl fragments of the phospholipids was determined by the formula:

$$S_{CH} = \frac{1}{2}\langle 3\cos^2\theta_i - 1\rangle,$$

where θ_i is the angle between the C–H bond at the ith carbon atom in the alkyl chain of the phospholipid and the normal to the membrane, while the figures in broken brackets designate time averaging. The maximum value of this parameter (when all bonds are parallel to the normal to the membrane) is equal to unity, the minimum value (when all bonds lie in the plane of the membrane) is –0.5. The calculated values of $-S_{CH}$ for the oleoyl chain manifest themselves as a characteristic depression near the double bond.

Dissipative characteristics of lipid membranes and diffusion of small molecules. Formamide, ammonia, water, oxygen, glycerol, ethanediol, ethanol, butyric acid, and urea were studied as candidate ligands

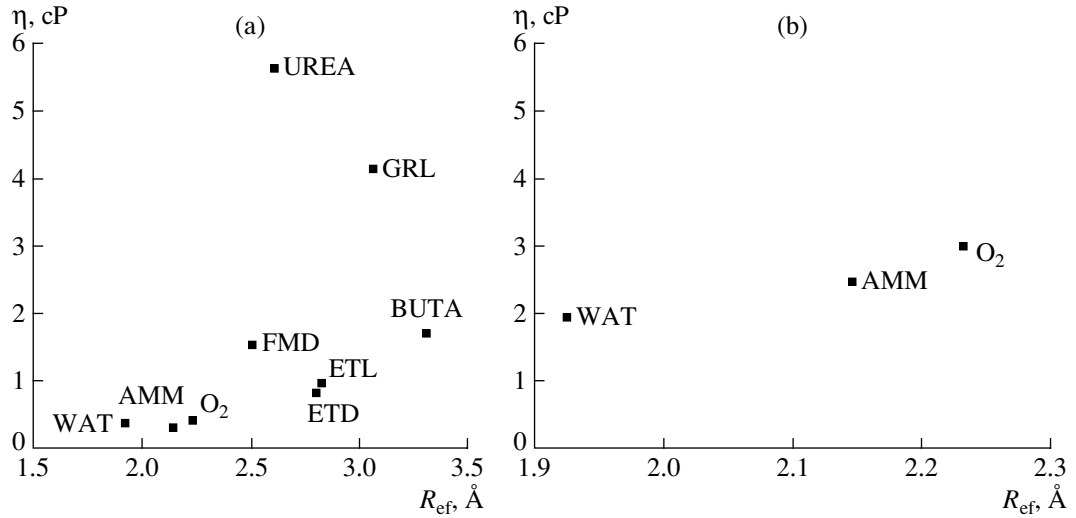

Fig. 6. Dependence of microviscosity on effective radius R_{ef} in the POPC–water system. Total F_{ext} = 10 kcal/mol Å^{-1}; (a) 6 kcal/mol Å^{-1}; (b) 2 kcal/mol Å^{-1}. Designations: WAT, water; AMM, ammonia; O_2, molecular oxygen; FMD, formamide; ETD, ethanediol; ETL, ethanol; UREA, urea; GRL, glycerol; BUTA, butyric acid.

(penetrants) using steered molecular dynamics simulation as a method of choice [20, 21]. Additional potential was superimposed on the system in order to stimulate its translocation along selected degrees of freedom.

A constant potential (2 and 6 kcal/mol Å^{-1}) applied to aqueous solutions of tested compounds was oriented along the normal in the direction of membrane surface. In the latter case (6 kcal/mol Å^{-1}), the measurements were performed in triplicate. The force was applied uniformly to all atoms of the ligand. The simulations were run till the first full penetration of ligand molecules into the membrane, but no longer than 2 ns. Displacement of ligand molecules was assessed by drift. Diffusion was not taken into consideration; local friction coefficients were determined as a ratio of applied force to drift velocity:

$$\gamma = \frac{F_{ext}}{\nu}.$$

The friction coefficient may conveniently be expressed as medium microviscosity using the Stokes formula or as a diffusion coefficient using the Einstein relation:

$$F = \frac{k_b T}{\gamma} = \frac{k_b T}{6\pi\eta r}.$$

The factors responsible for the significant deviation of true values from the Stokes hydrodynamic formula were described in our previous publication [17]. Interestingly, the Stokes ratio was found to be qualitatively more efficient even at the microlevel [40].

As was discussed previously [17], there exists a certain critical level of superimposed force, which favors transmembrane transfer of particles into the membrane in the course of nanoseconds (e.g., 1 kcal/mol Å^{-1} for 2A particles). The calculated values of effective viscosity descend at increasing force, which testify to non-newtonian origin of the medium and low non-equilibrium state of the experimental system at flow rates varying from 1 to 10 A/ps.

The dependences of effective microviscosities on ligand type and applied potential are shown in Fig. 6.

The higher the effective microviscosity of the lipid membrane at the given value of applied force, the lower the permeability of the membrane for ligand molecules. At 2 kcal/mol Å^{-1}, only very small molecules can penetrate into the membrane within a course of several nanoseconds, this time being too short for larger molecules to overcome the membrane barrier (Fig. 6b). Experimentally determined microviscosity values for membrane lipids vary from 30 to 190 cP depending on membrane type [41–43]. The corresponding value for POPC is of the order of 18 cP [44]. However, there is little or no evidence on microviscosities measured along the normal.

If ligand transport occurs in the hydrodynamic regime, membrane microviscosity does not depend either on the size or the chemical structure of the ligand molecule. Deviations can be induced by specific interactions between the ligand and the membrane (Fig. 6). A common feature is that the radius of the low-molecular ligand varies directly as the effective microviscosity of the membrane. This conclusion is in agreement with the increase in effective microviscosity, which is inversely correlated with the external force and, as a consequence, with the rate of ligand molecules transfer through the membrane. Special mention should be made of the drastic decrease in the permeability of membranes for urea, which can be attributed to strong dipole-dipole interactions creating local traps for urea molecules.

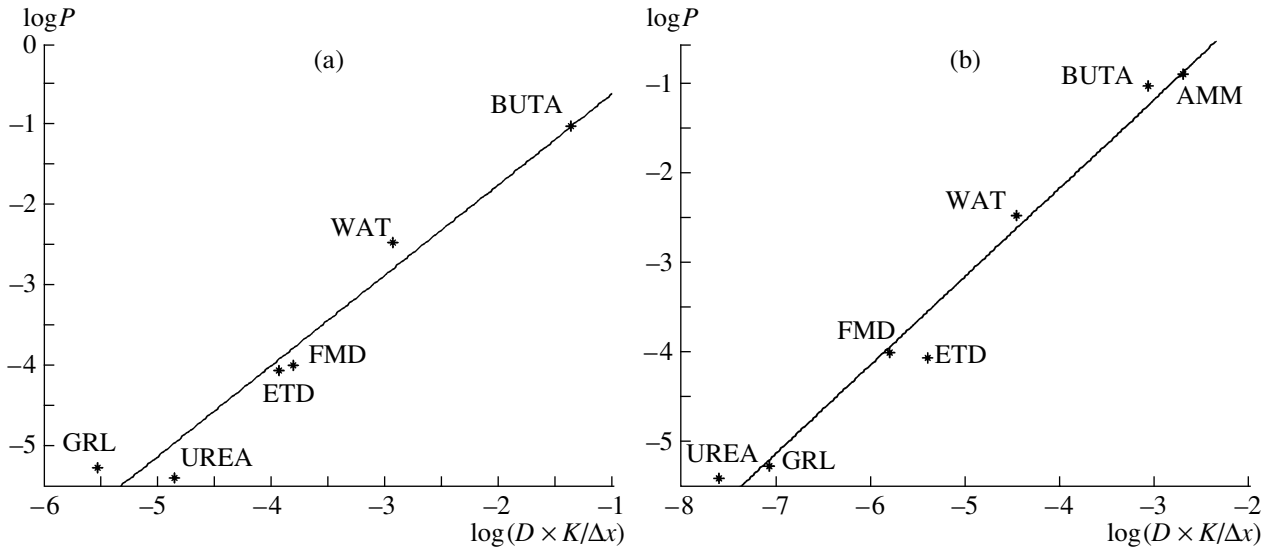

Fig. 7. Dependence of permeability P on $DK/\Delta x$, where D is the diffusion coefficient in the membrane, K is the distribution coefficient for the water–hydrophobic solvent system, and Δx is the membrane thickness (~40 Å). (a) Olive oil (correlation coefficient, 0.999); (b) hexadecane (correlation coefficient, 0.963). Designations as in Fig. 6.

A comparison of experimental mobility data reflecting the behavior of small molecules in hydrophobic solvents to experimental values of diffusion coefficients demonstrated that membrane permeability is a product of the diffusion coefficient and interfacial (membrane/water) distribution coefficient normalized by membrane thickness. Figure 7 illustrates conformity of the calculated interfacial distribution coefficients to experimentally determined values. As calculation of distribution coefficients is not a task in this particular case, the distribution coefficient of the penetrant was calculated from the corresponding values for water–hexadecane and water–olive oil systems [45]. The data obtained were consistent with the previously reported data on permeability of lipid membranes for ligand molecules. Noteworthy, the $DK/\Delta x$ values for the olive oil–water system showed a better correlation to the permeability P than those for the hexadecane–water system.

In this study, the MD approach based on the use of a standard molecular simulation protocol was employed for a comparison of major structural and kinetic parameters of fully hydrated POPC, DPPC and CL bilayers. The use of this protocol brings the system to local equilibrium and ensures easy distribution and stable characteristics of tested parameters.

The thickness of the membrane lipid bilayer, the distribution of atomic groups within the membrane relative to the normal, the radial distribution functions in the plane of the lipid bilayer and the order parameters of lipid chains are all consistent with experimental data. The design of collisional thermostats and Berendsen anisotropic barostats affords compensation for surface tension and natural parameterization errors imposed by the force field. The MD protocol used in this study enables acquisition of reasonable values of lateral diffusion coefficients and permeability of low-molecular ligands consistent with experimental data.

ACKNOWLEDGMENTS

The authors thank Dr. Yu.N. Antonenko for helpful discussions.

This work has been carried out with the financial support from the Federal Agency for Education, the Federal Agency for Science and Innovations and the Russian Foundation for Basic Research (grant nos. 06-04-08136 and 07-04-01169) and support from the U.S. Civilian Research and Development Foundation (grant no. 2803).

REFERENCES

1. Gennis, R.B., *Biomembrany: Molekuliarnaya struktura i funktsii* (Biomembranes: Molecular Structure and Function, New York: Springer-Verlag, 1989), Moscow: Mir, 1997.
2. Baker, R.W., Membrane Technology and Applications, N. Y.: McGraw-Hill, 1999.
3. Karplus, M. and McCammon, J., Molecular Dynamics Simulations of Biomolecules, *Nature Struct. Biol.*, 2002, vol. 9, pp. 646–652.
4. Frenkel, D. and Smit, B., Understanding Molecular Simulation: From Algorithms to Applications, 2nd ed., San Diego: Acad. Press, 2002.
5. Shaitan, K.V., Tourleigh, Ye.V., Golik, D.N., Tereshkina, K.B., Levtsova, O.V., Fedik, I.V., Shaytan, A.K., Li, A., and Kirpichnikov, M.P., Nonequilibrium Molecular Dynamics of Nanostructures Including Biological Ones, *Khim. Fizika* (Rus.), 2006, vol. 25, pp. 31–48.

6. Shaitan, K.V and Pustoshilov, P.P., Molecular Dynamics of Stearic Acid Monolayers, *Biofizika* (Rus.), 1999, vol. 44, pp. 429–434.
7. Balabaev, N.K., Rabinovich, A.L., Ripatti, P.O., and Kornilov, V.V., Molecular Dynamics of Polyunsaturated Lipid Monolayers, *Russ. J. Phys. Chem.* (Rus.), 1998, vol. 72, pp. 686–689.
8. Tourleigh, E.V., Shaitan, K.V., and Balabaev, N.K., Molecular Dynamics of Hydrated Hydrocarbon Membrane Structures, *Russ. J. Phys. Chem.* (Rus.), 2005, vol. 79, pp. 1448–1456.
9. Wataru, S., Keiko, S., Terujiko, B., and Masuhiro, M., Molecular Dynamics Study of Bipolar Tetraether Lipid Membranes, *Biophys. J.*, 2005, vol. 89, pp. 3195–3202.
10. Edholm, O. and Jahnig, F., The Structure of a Membrane-Spanning Polypeptide Studied by Molecular Dynamics, *Biophys. Chem.*, 1998, vol. 30, pp. 279–292.
11. Efremov, R.G., Volynsky, P.E., Nolde, D.E., Vergoten, G., and Arseniev, A.S., Implicit Two-Phase Solvation Model as a Tool to Assess Conformation and Energetics of Proteins in Membrane-Mimic Media, *Theor. Chem. Acc.*, 2001, vol. 106, pp. 48–54.
12. Stevens, M.J., Coarse-Grained Simulations of Lipid Bilayers, *J. Chem. Phys.*, 2004, vol. 121, pp. 11942–11948.
13. Essmann, U. and Berkowitz, M.L., Dynamical Properties of Phospholipid Bilayers from Computer Simulation, *Biophys. J.*, 1999, vol. 76, pp. 2081–2089.
14. Rog, T., Murzyn, K. and Pasenkiewicz-Gierula, M., Molecular Dynamics Simulations of Charged and Neutral Lipid Bilayers: Treatment of Electrostatic Interactions, *Acta Biochim. Pol.*, 2003, vol. 50, pp. 789–798.
15. Wang, J., Cieplak, P. and Kollman, P.A., How Well Does a Restrained Electrostatic Potential (RESP) Model Perform in Calculating Conformational Energies of Organic and Biological Molecules? *J. Comput. Chem.*, 2000, vol. 21, pp. 1049–1074.
16. Tourleigh, Ye.V., Shaitan, K.V., and Balabaev, N.K., Molecular Dynamics of a Hydrated Palmitoyloleoylphosphatidylcholine Bilayers in Collisional Thermostat, *Biologicheskie Membrany* (Rus.), 2005, vol. 22, pp. 519–530.
17. Tourleigh, Ye.V., Shaitan, K.V., and Balabaev, N.K., Dynamic Heterogeneity of Phospholipid Bilayer and Molecular Diffusion of Molecules at the Interface, *Biofizika* (Rus.), 2005, vol. 50, pp. 1042–1047.
18. White, S.H., Small Phospholipid Vesicles: Internal Pressure, Surface Tension, and Surface Free Energy, *Proc. Natl. Acad. Sci. USA*, 1980, vol. 77, pp. 4048–4050.
19. Orbach, E. and Finkelstein, A., The Nonelectrolyte Permeability of Planar Lipid Bilayer Membranes, *J. Gen. Physiol.*, 1980, vol. 75, pp. 427–436.
20. Park, S. and Schulten, K., Calculating Potentials of Mean Force from Steered Molecular Dynamics Simulations, *J. Chem. Phys.*, 2004, vol. 120, pp. 5946–5961.
21. Isralewitz, B., Gao, M., and Schulten, K., Steered Molecular Dynamics and Mechanical Functions of Proteins, *Curr. Opin. Struct. Biol.*, 2001, vol. 11, pp. 224–230.
22. Lemak, A.S. and Balabaev, N.K., A Comparison between Collisional Dynamics and Brownian Dynamics, *Mol. Simul.*, 1995, vol. 15, pp. 223–231.
23. Lemak, A.S. and Balabaev, N.K., Molecular Dynamics Simulation of a Polymer Chain in Solution by Collisional Dynamics Method, *J. Comput. Chem.*, 1996, vol. 17, pp. 1685–1695.
24. Murzyn, K., Rog, T., Jezierski, G., Takaoka, Y., and Pasenkiewicz-Gierula, M., Effects of Phospholipids Unsaturation on the Membrane/Water Interface: A Molecular Simulation Study, *Biophys. J.*, 2001, vol. 81, pp. 170–183.
25. Nichols-Smith, S., The, S.Y., and Kuhl, T.L., Thermodynamic and Mechanical Properties of Model Mitochondrial Membranes, *BBA Biomembranes*, 2004, vol. 1663, pp. 82–88.
26. Patrick, L., Martin, J.Z., and Benoit, R., Lipid-Mediated Interactions between Intrinsic Membrane Proteins: Dependence on Protein Size and Lipid Composition, *Biophys. J.*, 2001, vol. 81, pp. 276–284.
27. Hyslop, P.A., Morel, B., and Sauerheber, R.D., Organization and Interaction of Cholesterol and Phosphatidylcholine in Model Bilayer Membrane, *Biochemistry*, 1990, vol. 29, pp. 1025–1038.
28. Pabst, G., Rappolt, M., Amenitsch, H., and Laggner, P., Structural Information from Multilamellar Liposomes at Full Hydration: Full Q-Rangefitting with High Quality X-ray Data, *Phys. Rev. E*, 2000, vol. 62, pp. 4000–4009.
29. Smaby, J.M., Mornsen, M.M., Brockman, H.L., and Brown, R.E., Phosphatidylcholine Acyl Unsaturation Modulates the Decrease in Interfacial Elasticity Induced by Cholesterol, *Biophys. J.*, 1997, vol. 73, pp. 1492–1505.
30. Evans, R.W., Williams, M.A., and Tinoco, J., Surface Areas of 1-Palmitoyl Phosphatidylcholines and Their Interactions with Cholesterol, *Biochem. J.*, 1987, vol. 245, pp. 455–462.
31. Chiu, S.W., Clark, M., Balaji, V., Subramaniam, S., Scott, H.L., and Jakobsson, E., Incorporation of Surface Tension into Molecular Dynamics Simulation of Interface: A Fluid Phase Lipid Bilayer Membrane, *Biophys. J.*, 1995, vol. 69, pp. 1230–1245.
32. Braganza, L.F. and Worcester, D.L., Structural Changes in Lipid Bilayers and Biological Membranes Caused Hydrostatic Pressure, *Biochemistry*, 1986, vol. 25, pp. 7484–7488.
33. Sackmann, E., Handbook of Biological Physics, vol. 1A, Structure and Dynamics of Membranes, Lipowsky, R. and Sackmann, E., eds., Amsterdam: Elsevier, 1995, pp. 213–304.
34. Pfeiffer, W., Henkel, T., Sackmann, E., Knoll, W., and Richter, D., Local Dynamics of Lipid Bilayers Studied by Incoherent Quasi-Elastic Neutron Scattering, *Europhys. Lett.*, 1989, vol. 8, pp. 201–206.
35. Filippov, A., Oradd, G., and Lindblom, G., The Effect of Cholesterol on the Lateral Diffusion of Phospholipids in Oriented Bilayer, *Biophys. J.*, 2003, vol. 84, pp. 3079–3086.
36. Vaz, W.L.C. and Almeida, P.F., Microscopic Versus Macroscopic Diffusion in One-Component Fluid Phase Lipid Bilayer Membranes, *Biophys. J.*, 1991, vol. 60, pp. 1553–1554.
37. Schmidt, Th., Schutz, G.J., Baumgartner, W., Gruber, H.J., and Schindler, H., Imaging of Single Molecule Diffu-

sion, *Proc. Natl. Acad. Sci. USA*, 1996, vol. 93, pp. 2926–2929.

38. Nagle, J.F., Zhang, R., Tristram-Nagle, S., Sun, W.J., Petrache, H.I., and Suter, R.M., X-ray Structure Determination of Fully Hydrated L Alpha Phase Dipalmitoylphosphatidylcholine Bilayers, *Biophys. J.*, 1996, vol. 70, pp. 1419–1431.
39. Wiener, M.C. and White, S.H., Structure of a Fluid Dioleoylphosphatidylcholine Bilayer Determined by Joint Refinement of X-ray and Neutron Diffraction Data. III. Complete Structure, *Biophys. J.*, 1992, vol. 61, pp. 434–447.
40. Batchelor, G.K., Developments in Microhydrodynamics, Theoretical and Applied Mechanics, IUTAM Congress, Koiter, W.T., Ed., Amsterdam–New York–Oxford: North Holland–Elsevier Science Publishers, 1976, pp. 33–55.
41. Kung, C.E. and Reed, J.K., Microviscosity Measurements of Phospholipid Bilayers Using Fluorescent Dyes That Undergo Torsional Relaxation, *Biochemistry*, 1986, vol. 25, pp. 6114–6121.
42. Dunham, W.R., Sands, R.H., Klein, S.B., Duelli, E.A., Rhodes, L.M., and Marcelo, C.L., EPR Measurements Showing That Plasma Membrane Viscosity Can Vary from 30 to 100 cP in Human Epidermal Cell Strains, *Spectrochim. Acta A*, 1996, vol. 52, pp. 1357–1368.
43. Sinensky, M., Homeoviscous Adaptation–A Homeostatic Process That Regulates the Viscosity of Membrane Lipids in *Escherichia coli*, *Proc. Natl. Acad. Sci. USA*, 1974, vol. 71, pp. 522–525.
44. Sonnleitner, A., Schutz, G.J., and Schmidt, Th., Free Brownian Motion of Individual Lipid Molecules in Biomembranes, *Biophys. J.*, 1999, vol. 77, pp. 2638–2642.
45. Walter, A. and Gutknecht, J., Permeability of Small Nonelectrolytes through Lipid Bilayer Membranes, *J. Membr. Biol.*, 1986, vol. 90, pp. 207–217.